Two types of MGDG synthase genes, found widely in both 16:3 and 18:3 plants, differentially mediate galactolipid syntheses in photosynthetic and nonphotosynthetic tissues in *Arabidopsis thaliana*

Koichiro Awai*, Eric Maréchal†, Maryse A. Block†, Delphine Brun†, Tatsuru Masuda*, Hiroshi Shimada*, Ken-ichiro Takamiya*, Hiroyuki Ohta*, and Jacques Joyard†‡

*Graduate School of Bioscience and Biotechnology, Tokyo Institute of Technology, 4259 Nagatsuta, Midori-ku, Yokohama, Kanagawa 226-8501, Japan; and †Laboratoire de Physiologie Cellulaire Végétale, Unité Mixte de Recherche 5019 (Centre National de la Recherche Scientifique/Commissariat à l'Energie Atomique/Université Joseph Fourier), Commissariat à l'Energie Atomique, F-38054, Grenoble-Cédex 9, France

Communicated by Roland Douce, Universite de Grenoble, Grenoble, France, June 29, 2001 (received for review March 9, 2001)

In *Arabidopsis*, monogalactosyldiacylglycerol (MGDG) is synthesized by a multigenic family of MGDG synthases consisting of two types of enzymes differing in their N-terminal portion: type A (atMGD1) and type B (atMGD2 and atMGD3). The present paper compares type B isoforms with the enzymes of type A that are known to sit in the inner membrane of plastid envelope. The occurrence of types A and B in 16:3 and 18:3 plants shows that both types are not specialized isoforms for the prokaryotic and eukaryotic glycerolipid biosynthetic pathways. Type A *atMGD1* gene is abundantly expressed in green tissues and along plant development and encodes the most active enzyme. Its mature polypeptide is immunodetected in the envelope of chloroplasts from *Arabidopsis* leaves after cleavage of its transit peptide. atMGD1 is therefore likely devoted to the massive production of MGDG required to expand the inner envelope membrane and build up the thylakoids network. Transient expression of green fluorescent protein fusions in *Arabidopsis* leaves and *in vitro* import experiments show that type B precursors are targeted to plastids, owing to a different mechanism. Noncanonical addressing peptides, whose processing could not be assessed, are involved in the targeting of type B precursors, possibly to the outer envelope membrane where they might contribute to membrane expansion. Expression of type B enzymes was higher in nongreen tissues, i.e., in inflorescence (*atMGD2*) and roots (*atMGD3*), where they conceivably influence the eukaryotic structure prominence in MGDG. In addition, their expression of type B enzymes is enhanced under phosphate deprivation.

phosphate depletion | chloroplast envelope | UGT81A1 | UGT81A3 | UGT81A4

Galactolipids are a major class of higher plant glycerolipids because they are unique to plastid membranes from which they represent up to 80% of the total lipids (1). They contain one or two galactose molecules attached to the *sn*-3 position of a glycerol backbone, respectively monogalactosyldiacylglycerol (MGDG) and digalactosyldiacylglycerol (DGDG). In 16:3 plants,[§] two distinct pathways lead to the prokaryotic and eukaryotic *sn*-1,2-diacylglycerol (DAG) molecules, the substrates used to generate MGDG (1). The last step for MGDG biosynthesis is catalyzed by a UDP-galactose:*sn*-1,2-DAG 3-β-galactosyltransferase or MGDG synthase activity.

MGDG synthase activity was localized in the inner envelope membrane in spinach (a 16:3 plant) (3), whereas it was detected in the outer envelope membrane from pea (a 18:3 plant) (4). Further investigations in MGDG synthase localization were obviously limited by the lack of characterized polypeptides associated with the galactosylation activity. MGDG synthase encoding cDNAs were cloned in cucumber (5) and spinach (6). The encoded enzyme from spinach (soMGD1) could synthesize both prokaryotic and eukaryotic MGDG molecular species, and its processed form was imported in chloroplasts and immunodetected in the inner envelope membrane (6).

In *Arabidopsis*, at least two classes of MGDG synthase homologues can be distinguished according to the length of the N-terminal portion of the hypothetical precursors (6). Type A (atMGD1, csMGD1, and soMGD1) exhibits a ≈100-aa N-terminal peptide. A second type comprising atMGD2 and atMGD3, referred to as type B, has a shorter N-terminal sequence (≈40 aa) and no predictable targeting sequence.

In this paper, we question the rationale for a multigenic family of MGDG synthases. To that purpose we analyzed the substrate specificity of atMGD1, atMGD2, and atMGD3 from *Arabidopsis* in the context of the glycerolipid metabolism, compared the subcellular targeting and the processing of the nuclear encoded precursors, sought their precise localization in envelope membranes, and investigated their expression in various organs, along development, and under various growth conditions.

Materials and Methods

Isolation of *atMGD2* Coding Sequences by Screening cDNA and Genomic Libraries. A 1,647-bp fragment corresponding to the mature region of the cucumber MGDG synthase cDNA (5) was used as a probe to screen an *Arabidopsis* (Columbia) cDNA library constructed in λTI1 vector (7). Plaques grown on *Escherichia coli* LE392 were transferred to NYTRAN-N membranes (Schleicher & Schuell). Hybridization was carried out for 16 h at 55°C in 6× SSC (0.15 M NaCl and 15 mM sodium citrate), 5× Denhardt's solution, 0.1% (wt/vol) SDS, 100 μg/ml denatured salmon sperm DNA, and 10 ng of cucumber cDNA fragment labeled with α^{32}P-dCTP (ICN). Membranes were washed twice for 15 min at 55°C in 2× SSC, 0.1% (wt/vol) SDS, and then

Abbreviations: CHAPS, 3[(3-cholamidopropyl)-dimethylammonio]-1-propanesulfonate; DAG, diacylglycerol; DGDG, digalactosyldiacylglycerol; MGDG, monogalactosyldiacylglycerol; RT, reverse transcriptase; GFP, green fluorescent protein; UTR, untranslated region; EST, expressed sequence tag.

Data deposition: The sequences reported in this paper have been deposited in the GenBank database (accession nos. AL031004, AJ000331, AC007187, AB047475, and AB047476).

‡To whom reprint requests should be addressed. E-mail: jjoyard@cea.fr.

§Higher plant MGDG consists of two main molecular species: the major one has 18:3 at both *sn*-1 and *sn*-2 positions of the glycerol backbone (18:3/18:3), the second with 16:3 fatty acid exclusively at the *sn*-2 position of the glycerol (18:3/16:3). The C18/C18 structure is found in all eukaryotic lipids. By contrast, the C18/C16 structure is similar to that of cyanobacteria glycerolipids and is called prokaryotic. Plants containing only eukaryotic MGDG (18:3/18:3) are called 18:3 plants, whereas others, such as *Arabidopsis*, also contain prokaryotic MGDG (18:3/16:3) and are called 16:3 plants (2).

The publication costs of this article were defrayed in part by page charge payment. This article must therefore be hereby marked "*advertisement*" in accordance with 18 U.S.C. §1734 solely to indicate this fact.

www.pnas.org/cgi/doi/10.1073/pnas.181331498

autoradiographed. One positive clone (1,126-bp cDNA fragment) was isolated out of 300,000 plaques and used to screen another cDNA library constructed from whole *Arabidopsis* (Columbia) plants. Membranes were hybridized and washed at 65°C. A unique sequence of 1,647 bp was identified. The corresponding gene sequence was obtained by screening an *Arabidopsis* (Columbia) genomic library constructed in λZAP II vector (Stratagene), by using a 5′ end cDNA fragment (524 bp) of atMGD2 cDNA as described (8).

Isolation of *atMGD1* and *atMGD3* cDNAs. Nucleic fragments of *atMGD1* and *atMGD3* were cloned by PCR from the cDNA library used in the second screening of atMGD2 (see above). The fragments were used as probes to obtain the full-length *atMGD1* and *atMGD3* cDNAs.

Primer Extension Analyses. Probes designed to hybridize downstream to the putative initiation sites from *atMGD1* (GATGGATTCAGGACGAGGGAGGACG), *atMGD2* (GGGTGTTTGGGTGAACGATT), and *atMGD3* (CACCTTCTCAGTGATTGAATCCGAC) were labeled with ^{32}P-ATP (ICN) by using the Megalabel procedure (Takara Shuzo, Kyoto). The primer extension reaction was performed as described (9).

RNA Expression Analyzes by Reverse Transcriptase (RT)–PCR. Levels of *atMGD* gene expression were assessed by a kinetic RT-PCR approach. Primer sets were selected in similar regions in the three genes, embracing an intron to discriminate from genomic DNA amplification (see Fig. 5, which is published as supporting information on the PNAS web site, www.pnas.org). Ubq10 was used as a control for constant expression (10). All tested genes are unique in the *Arabidopsis* genome and show the same linear amplification rate from 11 to 17 cycles (not shown). Single-strand DNA was synthesized from DNase-treated total RNA (500 ng) by using avian myeloblastosis virus RT (Takara) in the presence of oligo(dT) primer at 42°C for 30 min. Thirteen-cycle PCR aliquots were analyzed on agarose gels, blotted, and radio-labeled with specific probes corresponding to the amplified fragments.

Localization of atMGD1, atMGD2, and atMGD3 Translationally Fused to Green Fluorescent Protein (GFP). Three chimeric *atMGD-GFP* sequences were constructed in pUC18 vectors in which *atMGD1*, *atMGD2*, and *atMGD3* sequences were fused upstream and in-frame with *GFP S65T* gene (11, 12) under the control of the cauliflower mosaic virus 35S promoter. Three-week old seedlings of *Arabidopsis* (WS) grown under 10-hr photoperiod were bombarded with vector DNA-coated gold particles (1,350 psi) by using a Bio-Rad PDS-1000He Particle Delivery System under the manufacturer's instructions. After 16 h, sample leaves were viewed by confocal laser scanning microscopy (Leica, TCS-SP2). GFP and chlorophyll fluorescence were excited and collected sequentially (400 Hz line by line) by using 488 nm for GFP excitation and 543 nm for chlorophyll excitation. GFP emission was collected from 510 to 535 nm and chlorophyll emission from 600 to 700 nm.

Expression of *atMGD1*, *atMGD2*, and *atMGD3* cDNAs in *E. coli*. The complete sequences of *atMGD2* and *atMGD3* and the mature form of *atMGD1* (i.e., without the 105-aa transit peptide) were in the pET-Y3a plasmid (6). BL21 *E. coli* hosts were grown at 37°C under vigorous agitation until the OD_{600} reached 0.4. Expression of recombinant MGDG synthase was induced by addition of 0.4 mM isopropyl β-D-thiogalactoside, and the cultures were allowed to grow for 3.5 h at 28°C. Collected bacteria were stored at −80°C.

Purification of Recombinant MGDG Synthases. All of the operations were carried out at 4°C. Pellets of recombinant bacteria were suspended in medium HA [6 mM 3[(3-cholamidopropyl)-dimethylammonio]-1-propanesulfonate (CHAPS), 50 mM Mops-NaOH (pH 7.8), 1 mM DTT] containing 50 mM KH_2PO_4/K_2HPO_4 at a final protein concentration of 0.8 mg/ml. The mixture was centrifuged for 15 min at 243,000 × *g* (Beckman L2, rotor SW 40). The supernatant containing solubilized proteins (16 mg) was loaded on a hydroxy-apatite-Ultrogel (IBF, Villeneuve-la-Garenne, France) column (Amersham Pharmacia column C10/20, 25 ml of gel), equilibrated with medium HA containing 50 mM KH_2PO_4/K_2HPO_4. The proteins were eluted by using a 50–275 mM KH_2PO_4/K_2HPO_4 gradient (in medium HA; flow rate, 30 ml/hr; fraction size, 1.5 ml). Recombinant MGDG synthases were eluted at 275 mM KH_2PO_4/K_2HPO_4 (see Fig. 6*B*, which is published as supporting information).

Polyclonal Antibody Production and Western Blot Analyses. Bacterial inclusion bodies enriched in recombinant MGDG synthases were used to obtain rabbit polyclonal antibodies (Elevage Scientifique des Dombes, Châtillon-sur-Chalaronne, France). Western blot analyses were performed by using several *Arabidopsis* and transformed *E. coli* subcellular fractions. Proteins (15–50 μg) were separated by SDS/PAGE on a 12% acrylamide gel and Western blot analyses were performed as described (13). MGDG synthase was detected with antibodies at a 1/5,000 dilution by using secondary antibodies coupled to alkaline phosphatase or horseradish peroxidase. Preimmune sera gave no signal.

Isolation of Chloroplast Envelope Membranes from *A. thaliana* Leaves. *A. thaliana* (WS) plants were grown for 6 weeks under a 10-hr photoperiod. Freshly collected leaves (300 g) were homogenized in 1.5 liters of ice-cold 0.45 M sorbitol, 20 mM Tricine-NaOH (pH 8.4), 10 mM EDTA, 10 mM $NaHCO_3$, 0.1% BSA. Crude chloroplast pellets obtained by centrifugation at 1,500 × *g* for 3 min were purified in 0.33 M sorbitol, 20 mM Mops (pH 7.6), 5 mM $MgCl_2$, 2.5 mM EDTA (buffer A) on a Percoll gradient formerly prepared by centrifugation of 45% Percoll in a SS 90 (Sorvall) vertical rotor at 10,000 × *g* for 100 min. After a 10-min centrifugation at 5,000 × *g*, intact chloroplasts were recovered as a heavy green layer, washed twice in buffer A, and broken in 10 mM Mops (pH 7.6), 4 mM $MgCl_2$, 1 mM PMSF, 1 mM caproic acid. Chloroplast subfractions were separated on a step gradient of 0.93 M–0.6 M sucrose in 10 mM Mops (pH 7.6) by centrifugation at 70,000 × *g* for 1 h. Envelope was collected at the interface between 0.6 M and 0.93 M sucrose layers.

Synthesis of *sn*-1,2-DAG Molecular Species. *sn*-1,2-Dilinoleoylglycerol (C18:2/C18:2) and 1-oleoyl-2-palmitoyl-*sn*-glycerol (C18:1/C16:0) molecular species were obtained after phospholipase C hydrolysis of phosphatidylcholine as described (14). *sn*-1,2-Dioleoylglycerol (18:1/18:1) was purchased from Sigma.

MGDG Synthase Assays and Kinetic Analyzes Using the Surface Dilution Model. MGDG synthase activity was assayed in several types of samples (see Fig. 6). Activity in membranes from recombinant *E. coli* was assayed as described (6). When CHAPS-solubilized recombinant MGDG synthases were purified by hydoxyapatite chromatography, we used mixed micelles (14) to fit the validation conditions of the "surface dilution" enzymology model (15). We determined that 0.117 mM, 1.864 mM, and 0.932 mM phosphatidylglycerol were broad optimum concentrations to assay the galactosylation activity in purified fraction of atMGD1, atMGD2, and atMGD3, respectively. Optimum pH were broad, pH 7.5 for both atMGD1 and atMGD3 and pH 8 for atMGD2. Therefore, enzymatic activities were compared at pH 7.8.

Lipids Extraction and Fatty Acid Analysis. Extractions of lipids were performed according to ref. 16. A powder obtained after grinding *Arabidopsis* seedlings under liquid nitrogen was macerated and extracted twice with 3 vol of chloroform/methanol (1:2,

vol/vol) by using mortar and pestle. After centrifugation at 1,600 × *g* for 5 min, the lower phases were recovered and the extract was evaporated. Residues were dissolved in chloroform/methanol (2:1, vol/vol) and stored at −30°C until use. The lipids were separated by two-dimensional TLC by using 7 M chloroform/methanol/ammonium (60:40:4) and chloroform/methanol/acetic acid/water (170:20:20:3) as solvents. For the analysis of galactolipids molecular species, a lipase from *Rhizopus delemar* was used as described (17). Fatty acid composition of galactolipids was determined by gas chromatography.

Results

Organization of *atMGD1*, *atMGD2*, and *atMGD3* Genes and Transcripts. Both *atMGD1* and *atMGD3* sequences were identified from *Arabidopsis* genome sequencing programs, in chromosomes IV and II, respectively. In addition, we screened *Arabidopsis* cDNA and genomic libraries and identified a third gene, *atMGD2*, held by chromosome V. Unexpectedly long 5′ untranslated regions (UTRs) were detected by primer extension analyzes of *atMGD1* and *atMGD2*, respectively, at the level of uridine-442 and guanosine-316 upstream to the start codon, whereas the *atMGD3* 5′ end was mapped at the level of adenosine-74 (Fig. 7, which is published as supporting information). The positional organization of the eight exons from *atMGD1* and *atMGD3* (I-VIII, see Fig. 5) are similar. Interestingly, *atMGD2* lacks two introns (see Fig. 5*A*), suggesting that the ancestral sequences for *atMGD1* and *atMGD3* originated from an early divergence marked by a deep modification of the N-terminal region and that *atMGD2* likely originated from the duplication of an *atMGD3* ancestral sequence (Fig. 5*B*).

Functional Expression and Purification of Recombinant *Arabidopsis* MGDG Synthases in *E. coli*. We inserted the cDNA fragments corresponding to the mature form of atMGD1 (46.87 kDa), i.e., truncated from its 105-aa chloroplastic transit peptide, and the full-length atMGD2 (52.73 kDa) and atMGD3 (52.86 kDa) into the pET-Y3a expression vector. Fig. 6*A* shows that the *E. coli* extracts expressing the *atMGD* cDNAs exhibit a galactosylation activity when provided with *sn*-1,2-dioleoylglycerol. We checked that the reaction product was MGDG by two-dimensional TLC as described (6) (not shown).

Enzymological comparisons require a purification of the properly folded enzymes. In addition, MGDG synthases must be extracted from the bacterial lipids to monitor the supply of DAG. Recombinant *E. coli* membranes were therefore solubilized by 6 mM CHAPS, under conditions defined (18). The specific activity increased after solubilization by the detergent: the enrichment factor for atMGD1 was 48, whereas it was more than 10 times lower for atMGD2 and atMGD3, respectively, 1.56 and 3.85. Solubilized fractions were subsequently chromatographed on a hydroxyapatite column under experimental conditions used for the purification of the spinach chloroplast envelope activity (6, 19). Most of the activity loaded on the column was recovered in a sharp peak eluted at 275 mM phosphate (Fig. 6*B*, peak III) with a yield of 45.2%, 13.1%, and 19.5% for atMGD1, atMGD2 and atMGD3, respectively and was used for enzymological comparisons.

Comparison of the Specificity of Recombinant atMGD1, atMGD2, and atMGD3 for Prokaryotic and Eukaryotic *sn*-1,2-DAG Molecular Species. The two DAG molecular species used to compare the specificity of the three MGDG synthases, i.e., *sn*-1-oleoyl,2-palmitoyl-glycerol (18:1/16:0) and *sn*-1,2-dilinoleoyl-glycerol (18:2/18:2), were chosen as physiologically relevant prokaryotic and eukaryotic molecular species. Using the surface dilution model (14), double reciprocal plots drawn for each DAG molecular species were linear (Fig. 6*C*) and used to calculate kinetic constants (Fig. 6*D*). The three enzymes are capable of synthesizing both prokaryotic and eukaryotic MGDG. Type B enzymes exhibit a higher affinity for eukaryotic DAG (18:2/18:2), possibly generated from extraplastidial glycerolipids, than for the molecular species abundantly produced inside the plastids (18:1/16:0). By contrast, the purified recombinant atMGD1 does not select the given substrates (Fig. 6*D*). Considering V_{max} and K_M values of the purified recombinant proteins, atMGD1 was the most active. V_{max} value is about five times higher than the values calculated for purified atMGD2 and atMGD3. In addition, atMGD1 used its substrates with the highest affinity: K_m values were about 0.0141 mol fraction for all substrates and were therefore lower than the best K_m values measured with 18:2/18:2 for atMGD2 and atMGD3 (Fig. 6*D*).

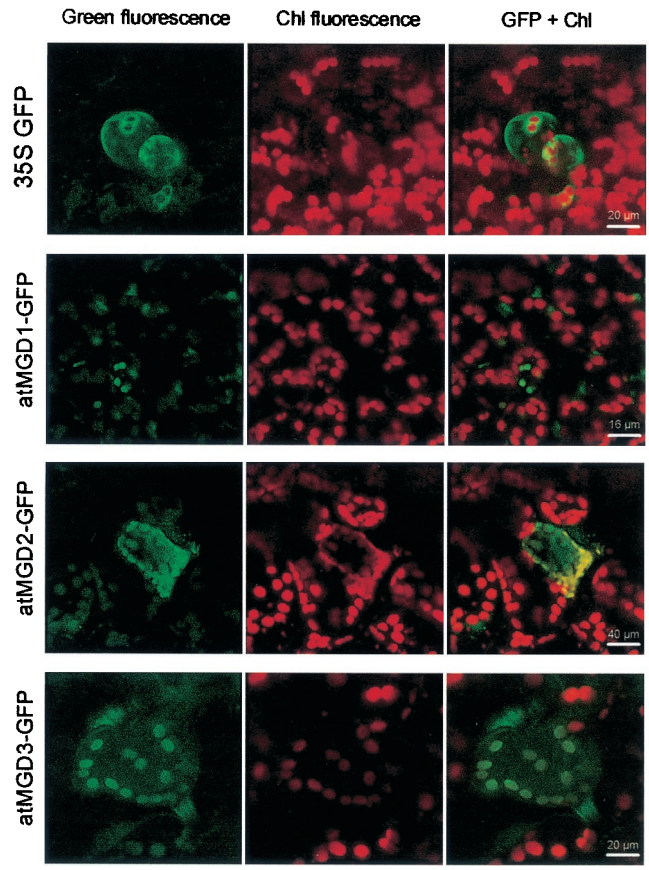

Fig. 1. Chloroplast localization of atMGD-GFP fusion after transient expression in rosette leaves of *Arabidopsis*. Expression of four constructs was analyzed: N-terminus fusions of *atMGD1* (atMGD1-GFP), *atMGD2* (atMGD2-GFP), or *atMGD3* (atMGD3-GFP) to the GFP sequence under the control of cauliflower mosaic virus 35S promoter and unfused GFP as a cytosolic control (35S GFP). GFP fluorescence (in green) was compared with chlorophyll autofluorescence (in red).

Import of atMGD1-GFP, atMGD2-GFP, and atMGD3-GFP Fusion Proteins into Chloroplasts. The enzymatic properties of the three isoforms may reflect a functional specialization to the DAG molecular species available in the membrane(s) where the enzymes sit (20). Because atMGD2 and atMGD3 did not exhibit any canonical chloroplastic transit peptide (6), we first investigated whether the full-length polypeptides contained functional addressing signals. Fig. 1 shows the green fluorescence emitted by GFP-fusion proteins transiently expressed in cells of *Arabidopsis* leaves observed by a confocal microscope. Chloroplasts were visualized by chlorophyll autofluorescence and appear in red at the periphery of cells. Without any fusion, GFP was localized randomly in the cytosol (Fig. 1, 35S GFP), whereas the

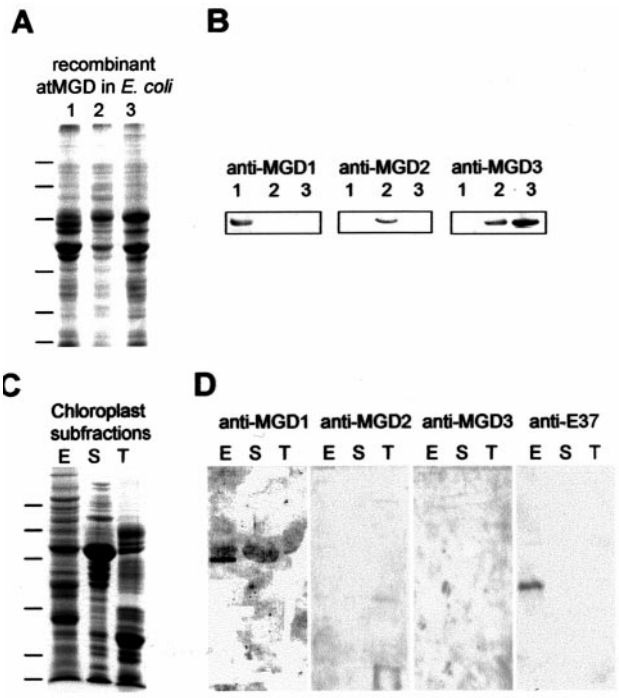

Fig. 2. Immunolocalization of atMGD1. The specificity of polyclonal antibodies prepared against atMGD1, atMGD2, and atMGD3 was first determined (*A* and *B*) and used to analyze the content of chloroplast subfractions (*C* and *D*). (*A*) Inclusion bodies enriched in atMGDs. Twenty five micrograms of protein was loaded in each lane and separated by SDS/PAGE. * indicate the positions of the overexpressed proteins. (*B*) Western blot analysis using 1:5,000-diluted primary antibodies. Detection was obtained after incubation with an secondary antibody linked to alkaline phosphatase. Anti-atMGD1 and anti-atMGD2 exhibit a high specificity, and anti-atMGD3 reacts with both atMGD2 and atMGD3. (*C*) Subfractions of *Arabidopsis* chloroplasts prepared from rosette leaves. Proteins (30 μg) from each chloroplast subfraction (E: envelope, S: stroma, T: thylakoids) were separated by SDS/PAGE. (*D*) Immunodetection of atMGD1 in chloroplast envelope membranes. Western blot using antibodies against atMGD1 (dilution 1:500), atMGD2 (dilution 1:500), atMGD3 (dilution 1:500), or E37, an envelope membrane marker (dilution 1:10,000) was carried out on E, S, and T lanes transferred to nitrocellulose. A polypeptide having a size consistent with the processed atMGD1 protein (type A) was detected. Type B enzymes are not detected. Positions of molecular mass standards (29, 33, 49, 82, and 105 kDa) are shown on the left.

N-terminal fusion to the transit peptide of the rubisco small subunit 1A led to an accumulated fluorescence in chloroplasts (data not shown). The full-length atMGD1 fused to the GFP is addressed to the chloroplast (Fig. 1, MGD1 GFP), as expected from the presence of a ≈100-aa N-terminal region similar to the cleaved chloroplastic transit peptide of csMGD1 and soMGD1 (5, 6). Likewise, the transient expression of both *atMGD2-GFP* and *atMGD3-GFP* chimeric cDNAs led to an accumulated green fluorescence in chloroplasts (Fig. 1, MGD2 GFP and MGD3 GFP, respectively). Together, these results indicate that the primary sequences of all three MGDG synthase precursors are sufficient to be addressed to plastids.

In addition, when incubated with chloroplasts isolated from pea leaves, radiolabeled precursors from atMGD1, atMGD2, and atMGD3 bound to chloroplasts (Fig. 8, which is published as supporting information). The atMGD1 precursor was processed into a polypeptide of 45 kDa and was subsequently protected from proteolytic treatment with thermolysin. For atMGD2 and atMGD3, the precursor binding to chloroplasts was strong, and we could not detect any cleavage product. After thermolysin treatment, when the full-length precursor of atMGD1 was completely hydrolyzed, a slight part of the

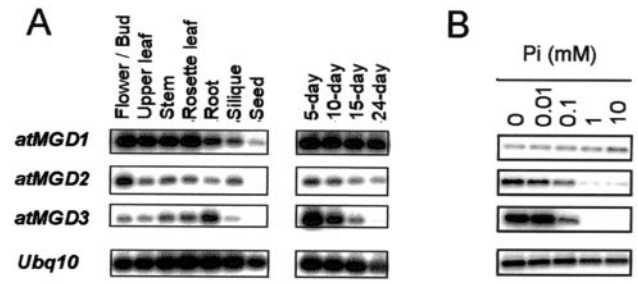

Fig. 3. Analyses of *atMGD* gene expression. (*A*) Expression of *atMGD* genes in various organs and developmental stages. (*B*) Expression of *atMGD* genes in total extracts from plants grown on Murashige and Skoog media supplemented with phosphate as indicated. RT-PCR analyses for *Arabidopsis MGD* genes were carried out as described in *Materials and Methods*. Amounts of DNA loaded per gel were adjusted for each experiment so as not to saturate the image.

atMGD2- and atMGD3-labeled proteins was found resistant to proteolysis (Fig. 8). These results indicated that precursors of atMGD2 and atMGD3 were imported into chloroplasts, confirming GFP-fusion experiments.

Immunodetection of atMGD1 in Chloroplast Subfractions. To localize the various MGDG synthases in cell subfractions, we prepared antibodies against each isoform. Fig. 2 *A* and *B* shows Western blot analyses made to estimate the cross-reactivity of the polyclonal antibodies. Very surprisingly, although the three proteins are very similar, polyclonal antibodies proved to be specific of the MGDG synthase against which it was produced (Fig. 2*B*), suggesting that immunogenic epitopes occurred mostly in nonconserved regions. Western blot analyzes carried out on total protein extract of different tissues of *Arabidopsis* did not allow any detection of MGDG synthases (data not shown). We sought whether any MGDG synthase could be detected in chloroplast envelope membranes purified from *Arabidopsis* and developed to that purpose, a procedure yielding 200 μg of purified chloroplast envelope membrane proteins by using 300 g of fresh *Arabidopsis* leaves (see *Materials and Methods*). Fig. 2 *C* and *D* shows a Western blot analysis of the polypeptides of *Arabidopsis* chloroplast envelope (E), stroma (S), and thylakoids (T). Accuracy of the subcellular fractionation was assessed by detection of E37, a marker for the inner envelope membrane (Fig. 2*D*). A polypeptide whose apparent molecular mass corresponds to the predicted mature atMGD1 (45 kDa) was detected in the envelope (Fig. 2*D*). By contrast, Fig. 2*D* does not show any immunodetection of atMGD2 or atMGD3. These results show that atMGD1 occurs abundantly in the envelope from leaf chloroplasts whereas atMGD2 and atMGD3 are either very minor or completely absent in this tissue.

Tissue- and Stage-Specific Expression of *MGD* Genes. We analyzed the mRNA expression levels of the three genes in major organs from *Arabidopsis* adult plants. Nonsaturated conditions for RT-PCR were set to achieve quantitative assays. As shown in Fig. 3*A*, *atMGD1* transcripts were dominantly detected in all organs examined, with little variations besides a lesser expression in siliques and a bare detection in seeds. By contrast, *atMGD2* and *atMGD3* expression levels were lower and detected especially in floral buds and roots, respectively. Distinct expression patterns were noticed along *Arabidopsis* seedling development (Fig. 3*A Right*). On one hand, *atMGD1* expression was detected dominantly throughout whole developmental stages, whereas expression of *atMGD2* was low and continuous. On the other hand, mRNA expression of *atMGD3* was most abundant in early stages, being quantitatively equal to that of *atMGD1*. Interestingly, under conditions of lowest expression of *atMGD1*, i.e., in roots and 5-day plants (Fig. 3*A*), the level of expression of type

A (*atMGD1*) is rather almost equal to that of type B (*atMGD2* + *atMGD3*).

Expression of *MGD* Genes under Phosphate Deprivation. Recently, Härtel *et al.* (21) described the accumulation of DGDG in extrachloroplast membranes in response to phosphate deprivation. Assuming that DGDG synthesis by this pathway requires MGDG synthesis, we compared expression of each *MGD* gene in plants grown under various phosphate concentrations (Fig. 3*B*). We observed that *atMGD1* expression remained almost constant, whereas expression of *atMGD2* and *atMGD3* increased under phosphate deprivation. These results indicate that type B enzymes could be devoted to a MGDG synthesis during phosphate deprivation and feed the DGDG synthesis presumed to replace missing phospholipids in extrachloroplast membranes.

Phylogenetic Occurrence of MGDG Synthase Genes of Types A and B in Higher Plants. The data collected in this study suggest that in *Arabidopsis* both type A and B enzymes can monitor MGDG synthesis from DAG originated either from the prokaryotic or eukaryotic pathways, being partially influential on the MGDG molecular species produced. We wondered whether the existence of type B was unique to *Arabidopsis*, especially if this type was also found in C18:3 plants. A basic BLAST screening (BLOSUM 62 matrix) of the GenBank expressed sequence tag (EST) database dbEST (22), using *atMGD2* as a probe, shows that members of type B MGDG synthases exist in numerous plant species. Fig. 4*A* shows a MULTALIN local alignment of 122-aa portions of the presently cloned full-length MGDG synthase sequences with screened ESTs. The corresponding phenogram (Fig. 4*B*) shows that the identified type A and B enzymes cluster in two distinct groups. Assuming that conserved amino acids in type A MGDG synthases, which are not conserved in type B, are signatures of type A (highlighted in black in Fig. 4*A*), this analysis shows an occurrence of type A in soybean, tomato, and barley. Vice versa, type B-specific amino acids (highlighted in gray in Fig. 4*A*) appear in soybean and lotus. Soybean is an example of a C18:3 plant harboring both types of MGDG synthases. Therefore, occurrence of both types A and B does not correlate with the classification according to the glycerolipid metabolism, i.e., coexistence of both prokaryotic and eukaryotic pathways in C16:3 plants and loss of the prokaryotic pathway in C18:3 plants. Fig. 4*C* shows the compiled results of local alignments of MGDG synthase ESTs exhibiting signatures of types A and B. Having found ESTs for MGDG synthases of types A and B in corn, the origin of both types precedes at least the monocotyledon divergence.

Discussion

MGDG synthase genes of types A and B are found widely in higher plants and are not related to the 16:3 or 18:3 plant categories (Fig. 4) and therefore to a hypothetical specialization in prokaryotic and eukaryotic glycerolipid syntheses. *Arabidopsis* and spinach enzymes of type A have been analyzed (5, 6), whereas the present paper also investigates type B isoforms. In *Arabidopsis, atMGD1*, *atMGD2*, and *atMGD3* encode polypeptides having a MGDG synthase activity *in vitro* (Fig. 1). Transcripts of *atMGD1* and *atMGD2* had relatively long 5′ UTRs, whereas in general, 5′ UTRs of plant mRNAs are shorter than 200 nt (23). We found that 5′ UTRs of *atMGD1* and *atMGD2* harbored 18- and 14-bp polypyrimidine tracts acting as possible internal ribosomal entry sites (24) at positions −25 to −8 for *atMGD1* and −131 to −118 for *atMGD2*. The analysis of insertion mutants in *atMGD1* gene supports the possible expression of transcripts of various sizes. A mutant of *atMGD1* gene, referred to as *mgd1–1* in the present paper (*mgd1* in ref. 25), was generated by a T-DNA tag insertion at position −148 upstream to the translation initiation codon and exhibits a 75% decrease in atMGD1 mRNA, a reduced leaf content of MGDG, a chlorotic phenotype, and strong defects in chloroplast ultrastructure (25).

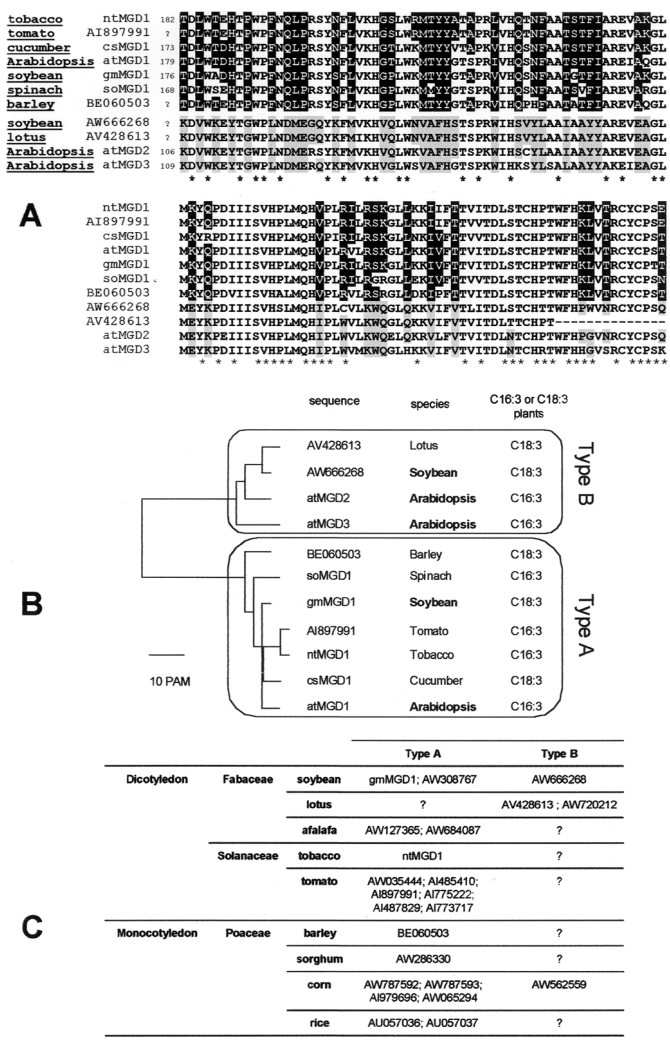

Fig. 4. Type A and type B MGDG synthases in the plant kingdom. A basic BLAST screening (BLOSUM 62 matrix) of the GenBank database dbEST, using *atMGD2* as a probe, led to the identification of putative MGDG synthases in various plant species. (*A*) Example of a local alignment. Identical amino acids are indicated by ⋆; amino acids that are common to cloned type A enzymes are highlighted in black whereas amino acids that are common to cloned type B enzymes (atMGD2 and atMGD3) are shown in gray. (*B*) Unrooted phenogram drawn by using the previous alignment. Distance is indicated in PAM (probability of accepted mutation). (*C*) Compiled results of local alignments of MGDG synthases ESTs exhibiting signatures of types A and B. Accession numbers of all ESTs are indicated.

After PCR screening of 10,000 lines from the Institut National de la Recherche Agronomique-Versailles collection (26), a close insertion mutant, named *mgd1–2*, was identified with a T-DNA inserted at position −214 (M.A.B., unpublished data). This second mutant does not show any peculiar phenotype under normal growth conditions. The phenotypes of *mgd1–1* and *mgd1–2* mutants indicate that the longest UTR (−442) is not necessary for an accurate atMGD1 expression under normal growth conditions. The decreased synthesis of MGDG in *mgd1–1* also correlates with the transcription of a shortest UTR, whose quantity and/or stability may be limiting. In addition to a strong promoter power close to the initiation site, expression of transcripts of variable size is therefore possibly critical to control the level of atMGD1 *in vivo*. Interestingly, despite competitive efforts to screen for MGDG synthase mutants, no null mutation (by T-DNA tag insertion or antisense strategies) could be identified to date, suggesting that atMGD1 may be absolutely necessary.

All three enzymes could synthesize MGDG by using any of the DAG molecular species we provided (Fig. 6*C*). Jarvis *et al.* (25) reported previously that *mgd1–1* mutation affected accumulation of both prokaryotic and eukaryotic galactolipids. As expected, we found that the recombinant atMGD1 was not selective. In addition, recombinant atMGD1 used all substrates with an activity (V_{max}) and specificity ($1/K_m$) much higher than those measured for atMGD2 and atMGD3 (Fig. 6*D*). Together with the high level of *atMGD1* transcript (Fig. 3*A*) and transcription product in leaf chloroplast envelope membranes (Fig. 2*C*), our results show that atMGD1 is the major MGDG producer. The targeting of atMGD1 to plastids and the processing of the precursor after import (Figs. 1 and 8), the localization of the spinach homologue in the inner envelope membrane (6), the chlorotic phenotype of chloroplasts, and the integrity of etioplasts in the *mgd1–1* mutant (25) indicate that the massive production of MGDG by atMGD1 is dedicated at least to inner envelope expansion and thylakoids building up.

Like type A enzymes, atMGD2 and atMGD3 can use prokaryotic or eukaryotic DAG molecular species, but they are more selective, having a higher specificity for the eukaryotic substrate (18:2/18:2) than for the prokaryotic one (18:1/16:0). GFP-fusion analyses (Fig. 1) and *in vitro* import studies (Fig. 8) showed that all gene products could be imported into chloroplasts. Type B enzymes have a shorter N-terminal region, without any predictable canonical transit peptide according to the ChloroP neural network-based method (27) although we noticed limited features of targeting peptides such as amphiphilic helices (Fig. 9, which is published as supporting information) and an enrichment in hydroxylated residues. *In vitro* import experiments suggest that there is no transit peptide processing and that a minor part of labeled atMGD2 and atMGD3 could be protected from surface proteolytic treatment of chloroplasts (Fig. 8). These results suggest a possible localization of atMGD2 and atMGD3 in the outer envelope membrane and targeting by a pathway similar to that used for OM14 and/or LeHPL (28, 29). Both OM14 and LeHPL are outer envelope membrane proteins that are not processed to lower molecular weight forms. In pea leaves, some substantial MGDG synthase activity was found in the outer envelope fraction in addition to a major activity in the inner envelope (30). Our results are compatible with the involvement of type B enzymes into MGDG synthesis in the outer envelope membrane, possibly dedicated to the outer envelope expansion. In nongreen tissues, the equal expression of type A and B enzymes (Fig. 3*A*) could therefore reflect a roughly equal quantity of MGDG synthases in both membranes of plastid envelope.

Expression of *atMGD2* and *atMGD3* was detected mostly in nonphotosynthetic tissues where plastids are smaller, devoid of any thylakoids, and galactolipids are present in lower amount. The highest expression of *atMGD2* in inflorescence extracts (Fig. 3*A*) supports a possible importance in the development of flowers. We showed that, in standard conditions, *atMGD3* mRNA accumulated at a comparable level to *atMGD1* mRNA in 5-day-old plant and was barely detectable after growth (Fig. 3*A*). In mature seedling *atMGD3* was expressed mostly in roots (Fig. 3*A*). As atMGD3 was shown to prefer eukaryotic DAG (Fig. 6), we wondered whether the abundance of atMGD3 could be correlated to the relative abundance of eukaryotic species of MGDG in young seedlings and roots. In young seedlings we noticed a higher proportion of eukaryotic MGDG and DGDG (Fig. 10, which is published as supporting information). Likewise, in roots of mature *Arabidopsis*, no 16:3 fatty acids could be detected in galactolipids (31), as is usually the case for nongreen plastids (32). Assuming that the MGDG synthases' specificity accounts for the MGDG distribution, then the present study supports a key involvement of atMGD3 in the production of eukaryotic MGDG in young seedlings and roots.

In response to phosphate deprivation, expression of *atMGD2* and *atMGD3* was stimulated (Fig. 3*B*). Therefore, atMGD2 and atMGD3 are also likely involved in MGDG production necessary for DGDG biosynthesis during phosphate deprivation (21). Because DGDG synthesized by this pathway is mainly of eukaryotic structure, atMGD2 and atMGD3's higher affinity for eukaryotic DAG substrates would reasonably account for the fatty acid distribution in phosphate-induced DGDG production. In conclusion, the data accumulated in this comparative study strongly suggest that, by contrast with atMGD1, atMGD2 and atMGD3 might be located in the outer membrane of the plastid envelope, likely assigned to the outer membrane expansion, and controlled by developmental and external factors in processes that are prominent in nongreen tissues.

We thank Dr. D. Grunwald (confocal microscopy facility from Commissariat à l'Energie Atomique, Grenoble) for his helpful expertise. Preliminary confocal microscopy experiments were carried out with the help of Dr. Y. Usson. We are also grateful for Dr. Y. Niwa for providing the GFP vectors, Prof. K. Iba for λ T1 library, Prof. K. Shinozaki for cDNA libraries, and Dr. S. Takeshita for pPICT2 vector. This work was supported by a grant Emergence-1999 from the Conseil Régional Rhône-Alpes, and Grant-in-Aid for Scientific Research on Priority Area (no. 11640644) from the Ministry of Education Science and Culture of Japan.

1. Joyard, J., Maréchal, E., Block, M. A. & Douce, R. (1996) in *Membranes: Specialized Functions in Plants*, eds. Smallwood, M., Knox, P. & Bowles D. J. (BIOS Scientific, Oxford), pp. 179–194.
2. Heinz, E. (1977) in *Lipids and Lipid Polymers*, eds. Tevini, M. & Lichtenthaler, H. K. (Springer, Berlin), pp. 102–120.
3. Block, M. A., Dorne, A.-J., Joyard, J. & Douce, R. (1983) *J. Biol. Chem.* **258,** 13281–13286.
4. Cline, K. & Keegstra, K. (1983) *Plant Physiol.* **71,** 366–372.
5. Shimojima, M., Ohta, H., Iwamatsu, A., Masuda, T., Shioi, Y. & Takamiya, K. (1997) *Proc. Natl. Acad. Sci. USA* **94,** 333–337.
6. Miège, C., Maréchal, E., Shimojima, M., Awai, K., Block, M. A., Ohta, H., Takamiya, K., Douce, R. & Joyard, J. (1999) *Eur. J. Biochem.* **265,** 990–1001.
7. Fuse, T., Kodama, H., Hayashida, N., Shinozaki, K., Nishimura, M. & Iba, K. (1995) *Plant J.* **7,** 849–856.
8. Church, G. M. & Gilbert, W. (1984) *Proc. Natl. Acad. Sci. USA* **81,** 1991–1995.
9. McKnight, S. L. & Kingsbury, R. (1982) *Science* **217,** 316–324.
10. Sun, C. W. & Callis, J. (1997) *Plant J.* **11,** 1017–1027.
11. Heim, R., Cubitt, A. B. & Tsien, R. Y. (1995) *Nature (London)* **373,** 663–664.
12. Chiu, W.-L., Niwa, Y., Zeng, W., Hirano, T., Kobayashi, H. & Sheen, J. (1996) *Curr. Biol.* **6,** 325–330.
13. Teyssier, E., Block, M. A., Douce, R. & Joyard, J. (1996) *Plant J.* **10,** 903–912.
14. Maréchal, E., Miège, C., Block, M. A., Douce, R. & Joyard, J. (1995) *J. Biol. Chem.* **270,** 5714–5722.
15. Deems, R. A., Eaton, B. R. & Dennis, E. A. (1975) *J. Biol. Chem.* **250**, 9013–9020.
16. Bligh, E. G. & Dyer, W. J. (1959) *Can. J. Biochem. Physiol.* **37,** 911–917.
17. Fischer, W., Heinz, E. & Zeus, M. (1973) *Hoppe Seylers Z. Physiol. Chem.* **354,** 1115–1123.
18. Covès, J., Block, M. A., Joyard, J. & Douce, R. (1986) *FEBS Lett.* **208,** 401–406.
19. Maréchal, E., Block, M. A., Joyard, J. & Douce, R. (1991) *C. R. Acad. Sci. Paris* **313,** 521–528.
20. Miège, C. & Maréchal, E. (1999) *Plant Physiol. Biochem.* **37,** 795–808.
21. Härtel, H., Dörmann, P. & Benning, C. (2000) *Proc. Natl. Acad. Sci. USA* **97,** 10649–10654. (First Published September 5, 2000; 10.1073/pnas.180320497)
22. Corpet, F. (1988) *Nucleic Acids Res.* **16,** 10881–10890.
23. Pesole, G., Liuni, S., Grillo, G. & Saccone, C. (1997) *Gene* **205,** 95–102.
24. Shama, S. & Meyuhas, O. (1996) *Eur. J. Biochem.* **236,** 383–388.
25. Jarvis, P., Dörmann, P., Peto, C. A., Lutes, J., Benning, C. & Chory, J. (2000) *Proc. Natl. Acad. Sci. USA* **97,** 8175–8179. (First Published June 27, 2000; 10.1073/pnas.100132197)
26. Bechtold, N. & Pelletier, G. (1998) *Methods Mol. Biol.* **82,** 259–266.
27. Emanuelsson, O., Nielsen, H. & von Heijne, G. (1999) *Protein Sci.* **8,** 978–984.
28. Froehlich, J. E., Itoh, A. & Howes, G. A. (2001) *Plant Physiol.* **125,** 306–317.
29. Li, H. M., Moore, T. & Keegstra, K. (1991) *Plant Cell* **3,** 709–717.
30. Tietje, C. & Heinz, E. (1998) *Planta* **206,** 72–78.
31. Browse, J., McConn, M., James, D., Jr. & Miquel, M. (1993) *J. Biol. Chem.* **268,** 16345–16351.
32. Douce, R. & Joyard, J. (1990) *Annu. Rev. Cell Biol.* **6,** 173–216.